

# Stereocomplexed Materials Based on Poly(3-hexylthiophene)-*b*-poly(lactide) Block Copolymers: Synthesis by Organic Catalysis, Thermal Properties, and Microscopic Morphology

Georgy Grancharov,<sup>†</sup> Olivier Coulembier,<sup>\*,†</sup> Mathieu Surin,<sup>‡</sup> Roberto Lazzaroni,<sup>‡</sup> and Philippe Dubois<sup>†</sup>

<sup>†</sup>Laboratory of Polymeric and Composite Materials and <sup>‡</sup>Laboratory for Chemistry of Novel Materials, Center for Innovation and Research in Materials and Polymers (CIRMAP), University of Mons-UMONS, 20, Place du Parc, 7000 Mons, Belgium

Received June 2, 2010; Revised Manuscript Received September 14, 2010

**ABSTRACT:** A new approach to control the supramolecular organization of conjugated polymers is proposed, based on stereocomplex formation. It is illustrated by mixing polymer solutions of block copolymers, i.e., poly(3-hexylthiophene)-*b*-poly(L-lactide) and poly(3-hexylthiophene)-*b*-poly(D-lactide). The block copolymers were successfully synthesized via a three-step procedure including the use of metal-free organic catalysts in the ring-opening polymerization of L- and D-lactide. The thermal properties and microscopic morphology of stereocomplexed diblock copolymers show that the stereocomplexation of the polylactide blocks is able to prevent the crystallization of the regioregular poly(3-hexylthiophene) block into long-range ordered parallel fibrillar structures. Stereocomplexation is also observed when mixing poly-(D-lactide) homopolymer and poly(3-hexylthiophene)-*b*-poly(L-lactide) block copolymer.

## Introduction

Poly(3-hexylthiophene) (P3HT) has been intensively studied and progressively optimized over the past two decades,<sup>1–3</sup> as a potentially useful component in organic field-effect transistors,<sup>4–7</sup> solar cells,<sup>8–11</sup> chemical electronic sensors,<sup>12</sup> and light-emitting devices.<sup>13</sup> The interest for P3HT stems from the combination of high charge carrier mobility, chemically tunable electronic properties, and good solubility. While the first regioregular P3HTs with head-to-tail couplings of 50–80% were obtained chemically<sup>14,15</sup> and electrochemically,<sup>16</sup> the drastic improvement of the optoelectronic properties was reached via the introduction of controlled polymerization schemes pioneered by the groups of McCullough<sup>17</sup> and Rieke.<sup>18</sup> Recently, a method called Grignard metathesis (GRIM) providing highly regioregular P3HT with approximately 98–100% head-to-tail couplings, narrow polydispersity, and good end-group control was established by McCullough.<sup>19–21</sup> The synthesis of those highly regioregular P3HTs brought a dramatic enhancement of the electrical properties due to a planarization of the backbone,  $\pi$ -stacking of flat polymer chains, and formation of well-ordered lamellar assembly of the chains. Such well-defined and organized three-dimensional polycrystalline structures<sup>22–24</sup> provide efficient inter-chain and intrachain charge carrier pathways, leading to high mobility.

Besides those advances, the efficiency of end-group control of the P3HT chains now allows a number of block copolymers between P3HT “rod-like segments” and other polymers “coil-like segments” to be prepared and subsequently tested in organic electronic devices.<sup>25–28</sup> The addition of a second block not only seems to have an effect on the crystallinity of the conjugated materials but also leads to new morphological behavior. Recent preliminary findings have shown little difference in the film microstructure upon changing the nature of the second block, except in

the case of poly(2-vinylpyridine).<sup>26,28–31</sup> Copolymers with poly-(DL-lactide)<sup>32</sup> and poly(L-lactide)<sup>33</sup> were used as structure-directing agents to pattern conjugated materials into ordered nanostructures, followed by the selective removal of the polylactide moieties. By expanding the structure and characteristics of the nonconjugated blocks covalently bonded, a better understanding can be gained regarding how the nature of the second block affects the copolymer microscopic morphology and the optoelectronic properties. In this work, we propose a new approach to control the supramolecular organization of P3HT chains and the microscopic morphology of thin films based on the stereocomplexation between poly(L-lactide) and poly(D-lactide) chains, each of which is part of a block copolymer with P3HT.

Poly(lactide)s (PLA) are biodegradable, biocompatible, and easily erodible aliphatic polyesters, nontoxic to human body and environment, which are produced from renewable resources.<sup>34–36</sup> They have been used as biomedical materials for tissue regeneration, matrices for drug delivery systems, and alternatives for commercial polymeric materials to reduce the impact on the environment.<sup>37–39</sup> Since 1987 when Ikada et al. discovered the phenomenon of stereocomplexation or stereocomplex formation between optically active poly(L-lactide) (PLLA) and poly(D-lactide) (PDLA) homopolymers based on (*S*)-lactic acid (L-lactoyl) and (*R*)-lactic acid (D-lactoyl) repeating units,<sup>40</sup> numerous studies have been carried out, dealing with the formation, structure, properties, degradation, and applications of the PLA stereocomplexes.<sup>41</sup> Stereocomplexation of PLA appears when PLLA and PDLA are mixed in equimolar ratio between the partners, L-lactide and D-lactide units, in solution (solution cast) or in bulk (crystallization from the melt). Stereocomplexation gives rise to a polymer with entirely new crystalline structure possessing triangular lattice.<sup>42,43</sup> The new three-dimensional organization in the PLA stereocomplex improves the mechanical properties, the thermal resistance, and to some extent the hydrolytical stability of PLA-based materials. These improvements arise from a peculiarly strong interaction between L-lactoyl

\*Corresponding author. E-mail: Olivier.Coulembier@umons.ac.be.

and D-lactoyl units in the PLLA/PDLA stereocomplexes, which does not exist in the single PLLA or PDLA homopolymers.

In this paper, we report the synthesis, characterization, and stereocomplex formation of P3HT-*b*-PLLA and P3HT-*b*-PDLA copolymers. The synthesis procedure consisted of three steps. The first one comprises the preparation of regioregular P3HT block by the GRIM method. The second one relies on the modification of the end groups, leading to a hydroxyl-terminated polythiophene macroinitiator (P3HT-OH) which is used, in the last step, to initiate the ring-opening polymerization (ROP) of L- or D-lactide as catalyzed by metal-free organic catalysts.<sup>44</sup> The macromolecular parameters of the block copolymers were determined by <sup>1</sup>H NMR spectroscopy and size exclusion chromatography (SEC). The stereocomplexes of P3HT-*b*-PLLA and P3HT-*b*-PDLA diblock copolymers were prepared via solvent casting, and they were evidenced by differential scanning calorimetry (DSC), X-ray diffraction (XRD), and atomic force microscopy (AFM) investigation. The goal of the study is to understand how the stereocomplex formed between the PLA (co)polymer blocks affects the supramolecular organization of the P3HT block and its typical fibrillar microstructure.

## Experimental Section

**Synthesis of Regioregular Head-to-Tail Poly(3-hexylthiophene) with  $\alpha$ -Bromine and  $\omega$ -Hydrogen End Groups (P3HT).** To a dry 100 mL two-neck flask under a nitrogen atmosphere was charged 2-bromo-3-hexyl-5-iodothiophene (1.12 g, 3.00 mmol) prepared previously in 90% yield according to the synthetic procedure published in the literature.<sup>45,46</sup> After three azeotropic distillations by toluene, anhydrous THF (15 mL) was added via a syringe, and the solution was cooled down to 0 °C. Isopropylmagnesium chloride (iPr-MgCl, 2 M solution in THF, 1.50 mL, 3.00 mmol) was added via a syringe, and the mixture was stirred at 0 °C for 0.5 h. That mixture was transferred via a cannula to a flask containing a suspension of Ni(dppp)Cl<sub>2</sub> (37.9 mg, 0.07 mmol) in THF (15 mL). The polymerization was carried out at 5–10 °C for 24 h and was quenched by rapid addition of 5 M HCl (5 mL). After termination, the reaction was stirred for 0.5 h and precipitated in cold methanol. The product was washed well with methanol and hexane to afford a purple solid (375 mg, yield 75%). <sup>1</sup>H NMR (300 MHz, CDCl<sub>3</sub>): 6.97 (1H, s), 2.79 (2H, t), 1.69 (2H, quint), 1.50–1.36 (2H, m), 1.36–1.25 (4H, m), 0.90 (3H, t). <sup>13</sup>C NMR (75 MHz, CDCl<sub>3</sub>): 140.0, 133.9, 130.7, 128.8, 31.9, 30.7, 29.7, 29.5, 22.9, 14.4. FT-IR, cm<sup>-1</sup>: 724, 819, 1376, 1454, 1510, 1562, 2854, 2923, 2953. UV-vis (CHCl<sub>3</sub>), nm: 450. MALDI-ToF: mainly Br/H end-capped,  $m/z$  = [166n(repeat unit) + 79(Br) + 1(H)]. SEC:  $M_n$  = 7850 g/mol, PDI = 1.14.

**Modification of Regioregular Head-to-Tail Poly(3-hexylthiophene) to  $\alpha$ -Bromine and  $\omega$ -Hydroxyl Group Terminated Initiator (P3HT-OH).**  $\alpha$ -Bromine,  $\omega$ -hydrogen, end group-bearing P3HT ( $M_n$  = 7850, PDI = 1.14) (300 mg, 0.038 mmol) was dissolved in anhydrous toluene (~80 mL) under an inert atmosphere. *N,N*-Dimethylformamide (DMF) (1.2 mL, 15.5 mmol, ~400 equiv excess) and phosphorus oxychloride (POCl<sub>3</sub>) (1.4 mL, 15.3 mmol, ~400 equiv excess) were then added to the solution. The temperature was increased, and the reaction was stirred at 75 °C for 24 h. The solution was cooled down to room temperature, and 10 mL of saturated aqueous solution of sodium acetate was added carefully to quench the reaction. The mixture was stirred for another 4 h, poured in cold methanol, filtered, extracted with 3  $\times$  50 mL portions CHCl<sub>3</sub> from water, and dried. Next,  $\alpha$ -bromine and  $\omega$ -aldehyde end group bearing P3HT ( $M_n$  = 7850, PDI = 1.14) (300 mg, 0.038 mmol) was dissolved in anhydrous THF (90 mL) under an inert atmosphere, and NaBH<sub>4</sub> (powder) (0.0114 g, 0.304 mmol, ~8 equiv excess) was then added at 0 °C to the solution. The temperature was increased, and the reaction was stirred at room temperature for 1 h 30 min. After the reaction completion, the solvent (THF) was evaporated, and 10 mL of 1 N HCl was then added to

quench the excess of NaBH<sub>4</sub>. The obtained polymer was washed with water (2  $\times$  20 mL) and methanol (2  $\times$  20 mL), filtered, and dried (285 mg, yield 95%). <sup>1</sup>H NMR (300 MHz, CDCl<sub>3</sub>): 6.96 (1H, s), 4.76 (s, signal of small intensity for terminal -CH<sub>2</sub>OH group), 2.79 (2H, t), 1.69 (2H, quint), 1.50–1.36 (2H, m), 1.36–1.25 (4H, m), 0.90 (3H, t). FT-IR, cm<sup>-1</sup>: 724, 819, 1376, 1457, 1509, 1561, 2854, 2923, 2953. MALDI-ToF: mainly Br/CH<sub>2</sub>OH end-capped,  $m/z$  = [166n(repeat unit) + 79(Br) + 32(CH<sub>2</sub>OH)]. SEC:  $M_n$  = 7900 g/mol, PDI = 1.18.

**Synthesis of Poly(3-hexylthiophene)-*b*-poly(L-lactide) Block Copolymer (P3HT-*b*-PLLA).** To a dry 50 mL two-neck flask under a N<sub>2</sub> atmosphere was charged P3HT-OH (50 mg, 0.0063 mmol) and dried by three azeotropic distillations by anhydrous toluene. The flask was transferred inside a glovebox, and a solution (10 mg/mL in CHCl<sub>3</sub>) of the TBD catalyst was added (0.0087 mmol, 121  $\mu$ L, 2.5% of L-LA monomer). After that, anhydrous CHCl<sub>3</sub> (0.6 mL) was added to reach a final L-LA monomer concentration of 0.5 M. The molecular weight of the PLA block was chosen to be equal to that of the P3HT block used as macroinitiator, and consequently L-LA monomer (50 mg, 0.35 mmol) was added to the reaction. The flask was brought outside the glovebox, and the reaction was stirred at 50 °C under a N<sub>2</sub> atmosphere for 24 h. The obtained block copolymer (97 mg, yield 94%) was quenched by benzoic acid (~5 mg) and precipitated in cold methanol. <sup>1</sup>H NMR (300 MHz, CDCl<sub>3</sub>): 6.96 (1H, s, P3HT backbone), 5.25–5.00 (2.6H, m, PLA backbone), 2.78 (2H, t, P3HT backbone), 1.69 (2H, quint, P3HT backbone), 1.50–1.63 (7.8H, m, PLA backbone), 1.50–1.36 (2H, m, P3HT backbone), 1.36–1.25 (4H, m, P3HT backbone), 0.90 (3H, t, P3HT backbone). SEC:  $M_n$  = 14 600 g/mol, PDI = 1.48.

**Synthesis of Poly(3-hexylthiophene)-*b*-poly(D-lactide) Block Copolymer (P3HT-*b*-PDLA).** The procedure for block copolymerization of D-LA onto the P3HT macroinitiator is the same as described above for L-LA, but instead of TBD, DBU (0.0087 mmol, 133  $\mu$ L, 2.5% of D-LA monomer) was used as metal-free organic catalyst. The block copolymer (80 mg, yield 60%) was obtained. <sup>1</sup>H (300 MHz, CDCl<sub>3</sub>): 6.96 (1H, s, P3HT backbone), 5.25–5.00 (1.2H, m, PLA backbone), 2.78 (2H, t, P3HT backbone), 1.69 (2H, quint, P3HT backbone), 1.50–1.63 (3.6H, m, PLA backbone), 1.50–1.36 (2H, m, P3HT backbone), 1.36–1.25 (4H, m, P3HT backbone), 0.90 (3H, t, P3HT backbone). SEC:  $M_n$  = 11 350 g/mol, PDI = 1.33.

**Preparation of Stereocomplex Cast Films.** The stereocomplex formation was studied on thin films from the PLLA/PDLA, P3HT-*b*-PLLA/HPDLA, and P3HT-*b*-PLLA/P3HT-*b*-PDLA pairs, obtained by evaporation of the polymer solutions in dichloromethane (CH<sub>2</sub>Cl<sub>2</sub>) at room temperature. For that purpose, the (co)polymer pairs (0.025 g) were dissolved in CH<sub>2</sub>Cl<sub>2</sub> (2.5 mL); the obtained solutions were mixed under vigorous stirring at equimolar ratio between the polyester partners (L-LA and D-LA) with respect to the PLA block length and the total polymer concentration was maintained at 1 wt %. Then the solutions were cast on a flat glass Petri dish surface forming films for the purpose of DSC investigation, and the solvent was left to evaporate at room temperature for 24 h. After evaporation of the solvent at room temperature all films were dried at 80 °C under vacuum for another 24 h. Similar, the cast films were prepared on a glass substrate (20  $\times$  25 mm) suitable for XRD measurements. In the case of AFM analysis a mica substrate (15  $\times$  15 mm) was used, and the polymer solutions were diluted to a concentration of 0.01 wt %. Before AFM measurement all thin films were annealed in closed vessel with a saturated chloroform vapor for 12 h. For the sake of comparison, films were also prepared from the (co)polymers alone using the same procedure described above.

## Results and Discussion

**Synthesis and Characterization of P3HT-*b*-PLA Block Copolymers.** Poly(3-hexylthiophene)-*b*-poly(L-lactide) and poly(3-hexylthiophene)-*b*-poly(D-lactide) block copolymers were synthesized via a three-step procedure beginning with Grignard metathesis (GRIM) for the preparation of the P3HT

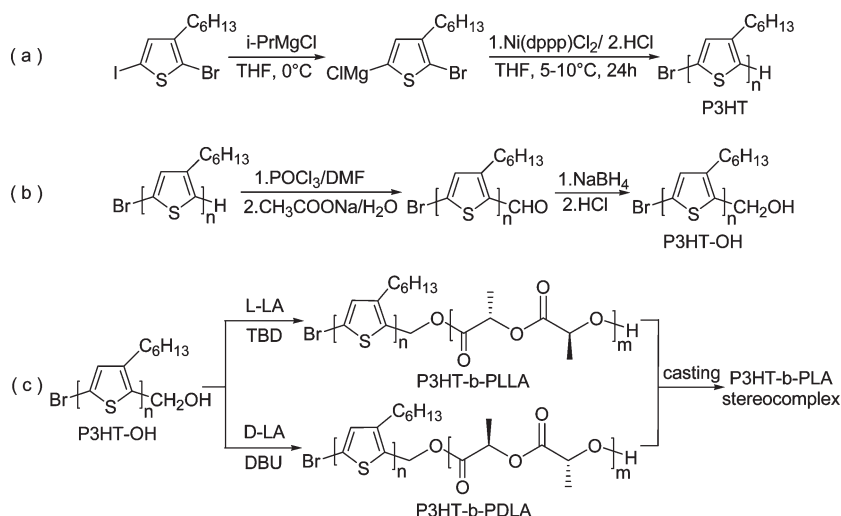
Scheme 1. Synthetic Route of P3HT-*b*-PLA Diblock Copolymers and Their Stereocomplexes

Table 1. Molecular Properties of the (Co)polymers

(co)polymer	$M_n^a$ (g/mol)	$M_n^a$ (g/mol) PLA bl	yield <sup>b</sup> (%)	$M_n^c$ exp (g/mol)	$M_n^d$ (g/mol)	PDI <sup>d</sup>
P3HT-OH	6320		75	7150	7900	1.18
P3HT- <i>b</i> -PLLA	14540	8220	94	15800	14600	1.48
P3HT- <i>b</i> -PDLA	10110	3790	60	15800	11350	1.33

<sup>a</sup>Number-average molecular weight of the (co)polymer and PLA block, as determined by  $^1\text{H}$  NMR spectroscopy in  $\text{CDCl}_3$ . <sup>b</sup>Determined gravimetrically after purification of the sample. <sup>c</sup>Expected number-average molecular weight of the (co)polymer. <sup>d</sup>Number-average molecular weight of the (co)polymer and polydispersity index, as determined by SEC in THF (+ 2 wt %  $\text{NEt}_3$ ) vs polystyrene standards.

block, followed by modification of this block to a hydroxyl-terminated poly(3-hexylthiophene) macroinitiator (P3HT-OH) and the ring-opening polymerization (ROP) of L- and D-lactide catalyzed by metal-free organic catalysts (Scheme 1).

The controlled GRIM method was used for the preparation of the well-defined regioregular head-to-tail P3HTs with tailored molecular weight and low polydispersity index (PDI).<sup>19–21</sup> The GRIM polymerization started with treating 2-bromo-3-hexyl-5-iodothiophene with 1 equiv of  $\text{iPr-MgCl}$ , resulting in a magnesium–iodine exchange reaction. The “Grignard intermediate” was then polymerized in the presence of  $\text{Ni(dppp)Cl}_2$  at a monomer-to-nickel catalyst molar ratio of 43:1, yielding a  $\alpha$ -bromo-poly(3-hexylthiophene) (Br-P3HT-H) similar to procedures described by McCullough and Yokozawa groups.<sup>19,45–47</sup> The polymerization was performed in cold THF ( $5–10^\circ\text{C}$ ) for 24 h and quickly terminated by instantaneous addition of 5 M HCl to prevent any trans-halogenation side reaction. Our observations showed that applying cold conditions during the GRIM polymerization produces poly(3-hexylthiophene)s that exhibit even lower PDI compared to those synthesized at room and higher temperatures (Table 1).<sup>45,48</sup>

Narrow PDIs associated with monomodal chromatograms attest for the good control over the GRIM polymerization. The high regioregularity content ( $>98\%$ ) was determined by  $^1\text{H}$  NMR (Figure 1) and FTIR, based on the standard calculations published in the literature,<sup>23</sup> while the presence of the expected end groups (H/Br) was fully evidenced by the signals at  $m/z = (166n + 79 + 1)$  in the MALDI-ToF spectrum.<sup>47</sup>

Two modification reactions were performed on the P3HTs to convert the bromide/hydrogen into bromide/methylol end groups. First, the bromide/aldehyde end groups were obtained quantitatively via the Vilsmeier–Haack reaction<sup>30</sup> which can be easily detected by the appearance of a strong band at  $1649\text{ cm}^{-1}$  in the FTIR spectrum, typical for the aldehyde group, and by the signals at  $m/z = (166n + 79 + 30)$  in the MALDI-ToF spectrum. Second, those bromide/aldehyde groups were converted to

bromide/methylol groups via a reduction reaction<sup>49</sup> by a selective and mild reagent such as sodium borohydride. The efficiency of the reaction was proven by the appearance of a  $-\text{CH}_2\text{OH}$  peak at 4.76 ppm in the  $^1\text{H}$  NMR spectrum (Figure 1a) and by the signals at  $m/z = (166n + 79 + 32)$  in the MALDI-ToF spectrum. The molecular weight of the P3HT-OH macroinitiator was also determined from the intensity of the  $-\text{CH}_2\text{OH}$  end group signal and will be used in all further steps (Table 1). The molecular weights were determined preferably via NMR due to the fact that SEC-calculated molecular weights of rodlike polymers (especially polythiophenes) vs polystyrene standards can be overestimated.<sup>50</sup>

Nonmetallic organic catalysts such as triazabicyclodecene (TBD) and diazabicycloundecene (DBU) were used for the ring-opening polymerization (ROP) of both L-lactide and D-lactide monomers from the P3HT-OH macroinitiator. The advantage of metal-free organic catalysts over well-known metal-containing tin and aluminum catalysts is obvious when the resulting polymer is likely to be applied in microelectronics and in living systems. For those applications, the obtained (co)polymer must be free of metal residues which are undesirable in the microelectronic devices and toxic for the organisms. Here we explored the procedure for macroinitiated ROP of L- and D-lactide by organic catalysts providing polymers of controlled molecular weight and polydispersity, similar to that described by Hedrick et al.<sup>51,52</sup> The reaction consists of treating the P3HT-OH macroinitiator with 2.5% (based on LA content) metal-free organic catalyst and addition of the LA monomer at a monomer-to-initiator molar ratio of 55:1. The polymerization was performed in  $\text{CHCl}_3$  at  $50^\circ\text{C}$  for 24 h and terminated by the addition of an excess of benzoic acid. The application of slightly elevated temperatures ( $50^\circ\text{C}$ ) during the block copolymerization reaction is absolutely necessary for the dissolution of the P3HT-OH macroinitiator and the controllable ROP of the lactide monomer. The  $^1\text{H}$  NMR spectra of the P3HT-*b*-PLLA and P3HT-*b*-PDLA block copolymers shown in parts b and c of Figure 1, respectively, display the complete disappearance of the



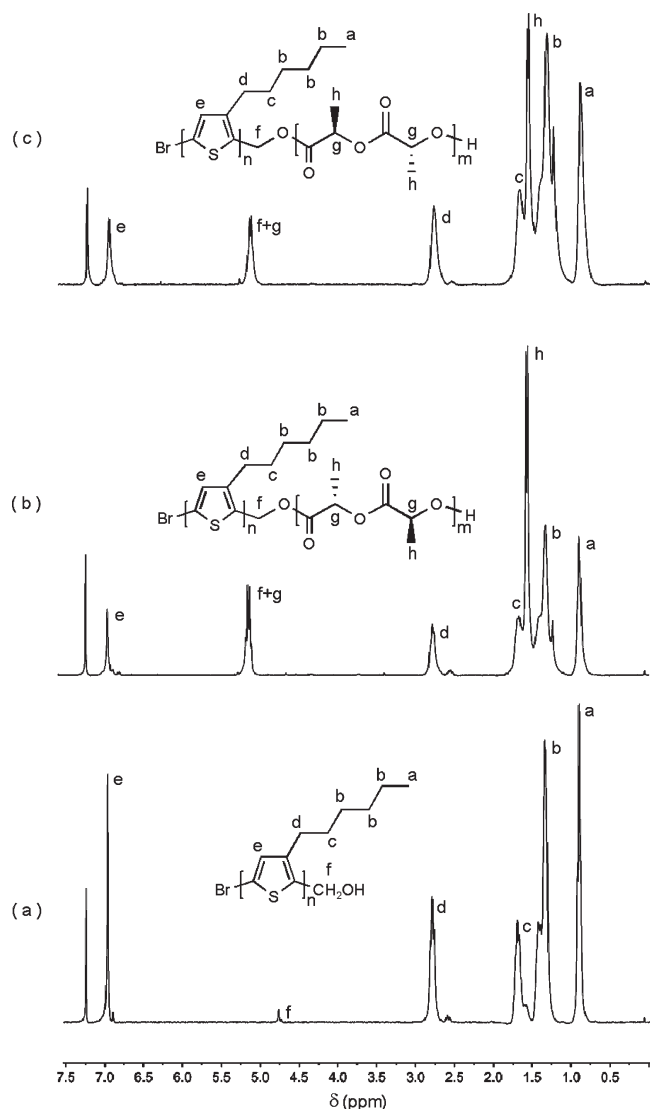


**Figure 1.**  $^1\text{H}$  NMR spectra of (a) P3HT–OH macroinitiator, (b) P3HT-*b*-PLLA block copolymer, and (c) P3HT-*b*-PDLA block copolymer.

weak signal at 4.76 ppm typical for  $-\text{CH}_2\text{OH}$  end group of the P3HT–OH macroinitiator and the appearance of new intense signals at 5.00–5.25 ppm for the methine groups of PLA and at 1.50–1.63 ppm for the methyl groups of PLA. The areas under these peaks were integrated, and the relative intensities were compared with the main-chain resonances associated with the P3HT chain to calculate the molecular weight of the PLA segment. Additional evidence for the synthesis of copolymers can be obtained from the data evaluated by SEC (Figure 2) which clearly shows the shift to lower elution volumes of the diblock copolymers compared to the trace initially recorded for the macroinitiator. Some increase of polydispersity with the length of PLA chain was found to be characteristic for that type of copolymers.<sup>32</sup> The low-molecular-weight tails observed on the traces could be explained by the presence of some remaining unreacted macroinitiator (or free polylactide chains).

It is known that the degree of stereocomplexation is affected by the molecular weight<sup>53</sup> of PLLA and PDLA chains: the stereocomplexation between polylactides of molecular weight higher than  $6 \times 10^4$  g/mol was proved to be hindered by homopolymer crystallization of the enantiomeric PLLA and PDLA polymers, while complete stereocomplexation can be observed for polylactide chains of sufficiently low molecular weights ( $< 4 \times 10^4$  g/mol). Thus, in order to facilitate the stereocomplexation of

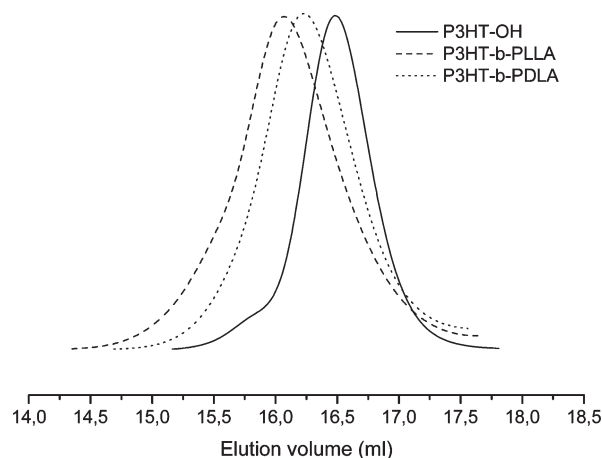


**Figure 2.** SEC traces of the P3HT–OH macroinitiator (solid line), P3HT-*b*-PLLA block copolymer (dashed line), and P3HT-*b*-PDLA block copolymer (dotted line) in THF (+ 2 wt %  $\text{NEt}_3$ ) as a mobile phase.

**Table 2.** Molecular Characteristic Features of the PLA Homopolymers

homopolymer	$M_n^a$ (g/mol)	yield <sup>b</sup> (%)	$M_n^c$ exp (g/mol)	$M_n^d$ (g/mol)	PDI <sup>d</sup>
PLLA	6770	75	7210	7150	1.49
PDLA	5040	90	7210	5400	1.26
HPDLA	9370	97	10670	10000	1.16

<sup>a</sup> Number-average molecular weight of the homopolymer, as determined by  $^1\text{H}$  NMR spectroscopy in  $\text{CDCl}_3$ . <sup>b</sup> Determined gravimetrically after purification of the sample. <sup>c</sup> Expected number-average molecular weight of the homopolymer. <sup>d</sup> Number-average molecular weight of the polymer and polydispersity index, as determined by SEC in THF (+ 2 wt %  $\text{NEt}_3$ ) vs polystyrene standards.

the PLA blocks, their targeted average molar mass was kept low: 8220 and 3790 g/mol for the PLLA block and the PDLA block, respectively (Table 1). For the same reason, the PLLA and PDLA homopolymers that were synthesized for the sake of comparison with the block copolymers have a molecular weight of 6770 and 5040 g/mol, respectively. A poly(D-lactide) homopolymer of higher molecular weight (HPDLA, 9370 g/mol) was also synthesized (Table 2).

The homopolymerization of L-LA and D-LA monomers was performed using 2-thiophenemethanol as initiator. That reaction proceeds in milder conditions because the application of elevated temperatures was not necessary. Room temperature was sufficient for the controllable ROP of the lactide monomers, and a lower amount of organic catalyst was used (only 0.5% based on LA content) compared with the block copolymerization.

**Thermal Analysis.** One of the most effective and simplest tools for monitoring PLA stereocomplexation is differential scanning calorimetry (DSC).<sup>41</sup> Stereocomplex formation was studied on cast films obtained by evaporation of polymer solutions in dichloromethane at room temperature. The following stereocomplex (co)polymer pairs PLLA/PDLA, P3HT-*b*-PLLA/P3HT-*b*-PDLA, and P3HT-*b*-PLLA/HPDLA were dissolved in  $\text{CH}_2\text{Cl}_2$ , mixed in equimolar ratio between the partners (L-LA and D-LA) with respect to the PLA block and then cast on a glass Petri dish surface. The total polymer concentration was maintained at 1 wt %, and solid films were obtained after drying. The thermal properties of the (co)polymers and related stereocomplexes are shown in Table 3.

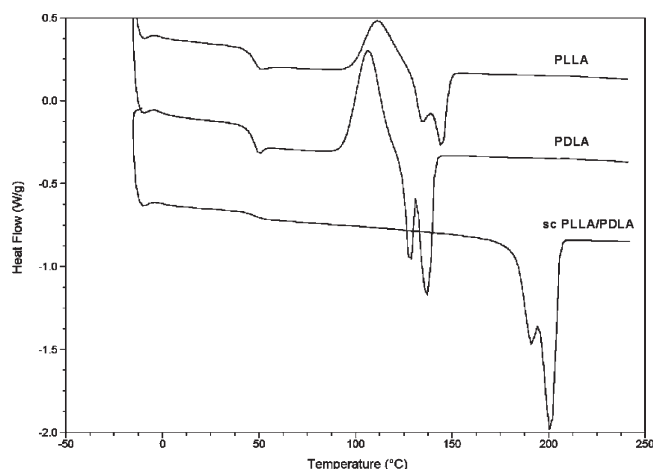
DSC analysis shows a melting temperature ( $T_m$ ) for the low-molecular-weight PLLA and PDLA homopolymers at 144 and 137 °C, respectively (Figure 3). The stereocomplex (sc) formed from the PDLA/PLLA pair shows a largely

**Table 3. Thermal Properties of the (Co)polymers and Their Respective Poly lactide Stereocomplexes**

sample <sup>a</sup>	$T_g$ (°C) PLA bl	$T_m$ (°C) PLA bl	$T_m$ (°C) P3HT bl	$\Delta H_m$ (J/g)
PLLA	51	144		32.5
PDLA	49	137		55
sc PLLA/PDLA	50	200		90
P3HT-OH <sup>b</sup>			202.5	20
P3HT- <i>b</i> -PLLA <sup>b</sup>	57	155	207.5	28 <sup>c</sup> 22 <sup>d</sup>
P3HT- <i>b</i> -PDLA <sup>b</sup>	45	145	197	24.5 <sup>c</sup> 10 <sup>d</sup>
sc P3HT- <i>b</i> -PLLA/ P3HT- <i>b</i> -PDLA <sup>b</sup>	55.5	203	41	
sc P3HT- <i>b</i> -PLLA/ HPDLA <sup>b</sup>	52	203	40	
mix P3HT- <i>b</i> -PLLA/ PLLA <sup>b</sup>	52	152	201.5	40 <sup>c</sup>

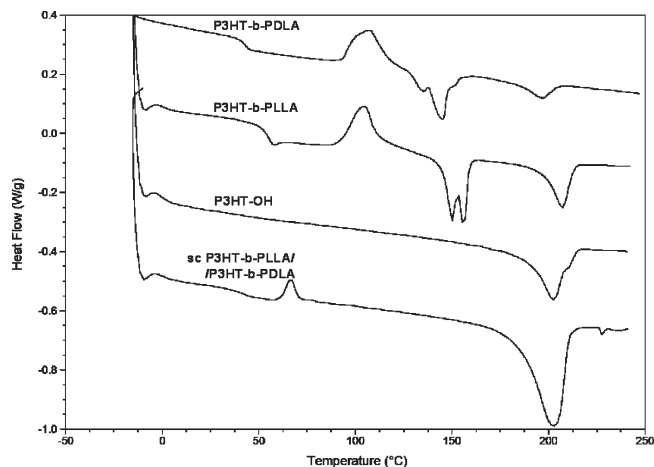
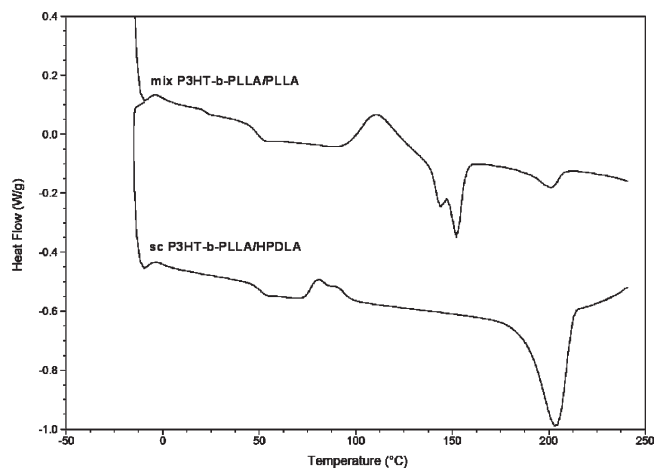
13<sup>d</sup>

<sup>a</sup>The samples were analyzed at a heating rate of 10 °C/min in a nitrogen flow. <sup>b</sup> $T_g$  of the P3HT block was too diffuse to be evaluated. <sup>c</sup> $\Delta H_m$  related to the melting of the PLA block. <sup>d</sup> $\Delta H_m$  related to the melting of the P3HT block.

**Figure 3.** DSC thermograms of PLLA homopolymer, PDLA homopolymer, and PLLA/PDLA stereocomplex measured at heating rate 10 °C/min.

increased  $T_m$  value at 200 °C, which is about 50–60 °C above the melting temperature of the initial PLLA and PDLA homopolymers. These results are in good agreement with the data published in literature for low-molecular-weight polylactides.<sup>54,55</sup> It is known that the melting enthalpy ( $\Delta H_m$ ) of infinity size crystals is different for polylactide homocrystallites (106 J/g)<sup>56</sup> compared to stereocomplex crystallites (142 J/g).<sup>57</sup> In the present study, the enthalpy value of the homopolymers is 32.5 J/g for PLLA and 55 J/g for PDLA, whereas the  $\Delta H_m$  of the PDLA/PLLA stereocomplex has a significantly higher value of 90 J/g.

The DSC analysis also indicates that the presence of the P3HT block does not impede the stereocomplex formation between the PLLA and PDLA segments in the copolymers. The film obtained from the combined solutions of the P3HT-*b*-PLLA/P3HT-*b*-PDLA diblock copolymers exhibit only one intense melting peak centered at 203 °C, very similar to that of the starting P3HT-OH macroinitiator (202.5 °C), very close to that of the PLLA/PDLA stereocomplex (200 °C) and, interestingly enough, significantly higher than the melting temperatures of the PLA blocks in the separate block copolymers (155 and 145 °C for the PLLA and PDLA block, respectively, Figure 4). This clearly indicates the existence of stereocomplex formation between the PLA segments in the combined solutions of the diblock copolymers.

**Figure 4.** DSC thermograms of P3HT-OH macroinitiator, P3HT-*b*-PLLA block copolymer, P3HT-*b*-PDLA block copolymer, and P3HT-*b*-PLLA/P3HT-*b*-PDLA stereocomplex measured at heating rate 10 °C/min.**Figure 5.** DSC thermograms of P3HT-*b*-PLLA/HPDLA stereocomplex and mixture of P3HT-*b*-PLLA/PLLA measured at heating rate 10 °C/min.

As can be seen from Table 3, the  $\Delta H_m$  values for copolymers P3HT-*b*-PLLA (22 J/g for the P3HT block and 28 J/g for the PLLA block), P3HT-*b*-PDLA (10 J/g for the P3HT block and 24.5 J/g for the PDLA block), and their stereocomplex (41 J/g) are lower compared to those of the homopolymers. This can be attributed to the presence of P3HT segments, which disturb the microstructural organization of the PLA segments into highly crystalline domains. At this stage, one cannot discriminate between the melting of the P3HT blocks and stereocomplexed PLA sequences since only one intense endotherm is observed at 203 °C.

Further investigations on the stereocomplex behavior of P3HT-*b*-PLA block copolymers showed that stereocomplexation can also be observed between the higher molecular weight poly(D-lactide) (HPDLA) homopolymer and the P3HT-*b*-PLLA diblock copolymer. The DSC thermogram shown in Figure 5 reveals that the melting temperature of the P3HT-*b*-PLLA/HPDLA film is again centered on 203 °C, and no trace of a  $T_m$  specific for individual PLLA or PDLA segments can be detected. For comparison, the mixture (mix) of the poly(L-lactide) homopolymer and the P3HT-*b*-PLLA diblock copolymer leads to the presence on the DSC thermogram of two melting temperatures typical for each component of the mixture: 201.5 °C for the crystalline P3HT segment and 152 °C for the PLLA segment in both the homopolymer and the copolymer (Figure 5).

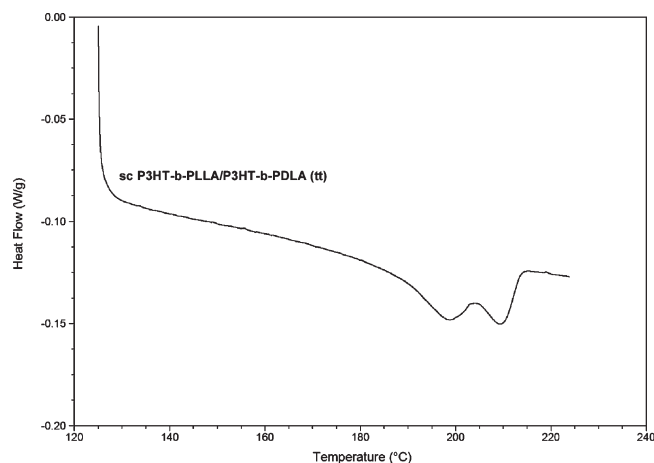


**Figure 6.** DSC thermograms of thermal treated stereocomplexes: P3HT-*b*-PLLA/P3HT-*b*-PDLA (tt) measured at heating rate 3 °C/min and in modulated temperature mode.

The melting signatures of both PLA stereocomplex and P3HT block are overlapping each other into one broad endotherm centered on 203 °C in all stereocomplexed samples, i.e., in the mixture of the two diblock copolymers and in the film of diblock copolymer added with the homopolymer. A successful way to resolve that strong endotherm into two separated peaks has been found out by applying a specific thermal treatment to the sample, decreasing the heating rate to 3 °C/min and using the modulated mode of DSC apparatus. The thermal treatment includes the melting of the polymer sample at a temperature of 225 °C, followed by cooling procedure to 125 °C. When cooled down, samples were kept for an additional hour at that temperature, allowing all stereocomplexed PLA chains to organize and crystallize.<sup>54</sup> The thermograms of thermally treated (tt) stereocomplexed samples P3HT-*b*-PLLA/P3HT-*b*-PDLA (tt) and P3HT-*b*-PLLA/HPDLA (tt) are shown in Figure 6. The sample based on P3HT-*b*-PLLA and P3HT-*b*-PDLA copolymers contains approximately the same quantity of PLA and P3HT segments and exhibits this time a clear separation of the melting peak into two components. The first one is centered on 198 °C and can be assigned to the stereocomplexed PLA segments, while the second melting situated at 209.5 °C corresponds to the P3HT blocks.

**X-ray Diffraction (XRD) Analysis.** The stereocomplex formation between the P3HT-*b*-PLLA/P3HT-*b*-PDLA copolymers, the PLLA/PDLA homopolymers, and the P3HT-*b*-PLLA/HPDLA copolymer/homopolymer pair was also studied by means of XRD. All XRD profiles are measured on films cast from methylene chloride solutions, in a  $2\theta$  interval from 4° to 30° and targeted signals are pointed by arrows (see Supporting Information, Figure S1). The PLLA and PDLA homopolymers show an identical diffraction profile: a strong signal at  $2\theta = 16.5^\circ$  for the (110)/(200) reflections and a weak signal at  $2\theta = 18.9^\circ$  for the (203) reflection. The diffraction peaks for the stereocomplexed PLLA/PDLA pair are situated at different  $2\theta$  positions, consistent with the different crystalline structure of the polymer complex. Those signals are a strong peak at  $2\theta = 11.8^\circ$  for the (100) reflection and weak signals at  $2\theta = 20.7^\circ$  and  $2\theta = 23.8^\circ$  for the (110) and (210) reflections, respectively. The XRD data for the PLA homopolymers and the stereocomplex based on them are in good agreement with the data published in literature.<sup>40,42,43,55</sup> The XRD profile of the P3HT-OH initiator shows the typical sequence of the (*n*00) reflections (with *n* = 1–3) for P3HT at  $2\theta = 5.4^\circ$ ,  $2\theta = 10.9^\circ$ , and  $2\theta = 16.7^\circ$ , with decreasing intensity, as previously observed by many authors.<sup>23,58,59</sup> The XRD patterns for the

two block copolymers, P3HT-*b*-PLLA and P3HT-*b*-PDLA, are very similar to that of the P3HT-OH macroinitiator. As far as the diffraction peaks of the polylactide blocks are concerned, the signal at  $2\theta = 16.6^\circ$  is more likely superimposed to the peak at the  $2\theta = 16.7^\circ$  assigned to the P3HT block as attested by its increased intensity. The diffraction peaks of the P3HT-*b*-PLLA/P3HT-*b*-PDLA stereocomplex are also situated at similar  $2\theta$  positions:  $2\theta = 5.4^\circ$  and  $2\theta = 10.8^\circ$  for the (100) and (200) reflections of the P3HT block, along with a new signal at  $2\theta = 11.8^\circ$  corresponding to the (100) reflection of the PLA stereocomplex. Besides the appearance of that signal at  $2\theta = 11.8^\circ$ , the existence of the PLA stereocomplex is also marked by the total disappearance of the signals at  $2\theta = 16.5^\circ$  typical for PLLA and PDLA blocks. Consistently, in the XRD profile of the P3HT-*b*-PLLA/HPDLA stereocomplex, all the peaks are situated as the sc P3HT-*b*-PLLA/P3HT-*b*-PDLA system, and the characteristic signal at  $2\theta = 11.8^\circ$  shows higher intensity due to the larger amount of PLA. In contrast, in the XRD pattern of the P3HT-*b*-PLLA/PLLA mixture, the peaks are at the same  $2\theta$  positions as in the pattern of the P3HT-*b*-PLLA block copolymer, and the signal at  $2\theta = 16.5^\circ$  is of higher intensity due to the contribution of crystalline PLA.

**Atomic Force Microscopy (AFM) Analysis.** The tapping-mode AFM phase images of P3HT-OH macroinitiator thin films show long-range parallel arrangement of fibrillar objects, which is the well-known morphological signature for most regioregular polyalkylthiophene homopolymers<sup>3,60</sup> (Figure 7a). Thin films of the P3HT-*b*-PLLA and P3HT-*b*-PDLA copolymers present similar long-range morphology (Figure 7b). These fibrillar objects are often referred to as nanoribbons and are typical for regioregular poly(3-alkylthiophene) crystallization. In P3HT-*b*-PLLA thin films, the average width of the fibrils is  $15 \pm 2$  nm, consistent with an assembly made of parallel  $\pi$ -stacked P3HT blocks perpendicular to the fibrils long axes and PLLA blocks in compact configuration on the edges of the P3HT lamellae, as in other rod-coil copolymers comprising P3HT rod block.<sup>25,26,29–33,61</sup> The long-range parallel ordering of fibrils in P3HT-*b*-PLLA films suggests that the crystallization of the P3HT block is barely disturbed by domains of the PLA block (only small areas show a different morphology visible as dark spots in Figure 7b). However, for the thin films of the P3HT-*b*-PLLA/P3HT-*b*-PDLA stereocomplex, the AFM images (Figure 7c) show that the long-range parallel arrangement of fibrils is clearly disturbed: even though a few hundreds nanometer long fibrils are still observed, these are isolated from each other and surrounded by a matrix showing no specific texture. That reveals that the stereocomplex crystal formation prevents the crystallization of P3HT to a certain extent.

To confirm this hypothesis, we studied thin films of blends of the P3HT-*b*-PLLA copolymer with the pure PLLA homopolymer (Figure 7d) and with the pure HPDLA homopolymer (Figure 7e). In the first case, only mixing without stereocomplexation occurs, and AFM shows parallel fibrils close-packed into large domains (similar to those of the diblock P3HT-*b*-PLLA copolymer), which are separated by dark untextured domains, probably containing the pure PLLA homopolymer. In the second case, stereocomplexation occurs, the fibrillar morphology disappears, and AFM shows a rather untextured morphology made of different domains which cannot be identified. Note that the morphology of pure PLLA and PDLA homopolymer thin films prepared in the same conditions also presents untextured morphologies (Figure 7f). Altogether, these results suggest that in copolymers or in blends the PLA stereocomplexation prevents the crystallization of regioregular P3HT into long-range parallel fibrillar domains and creates novel supramolecular organization in the thin films.



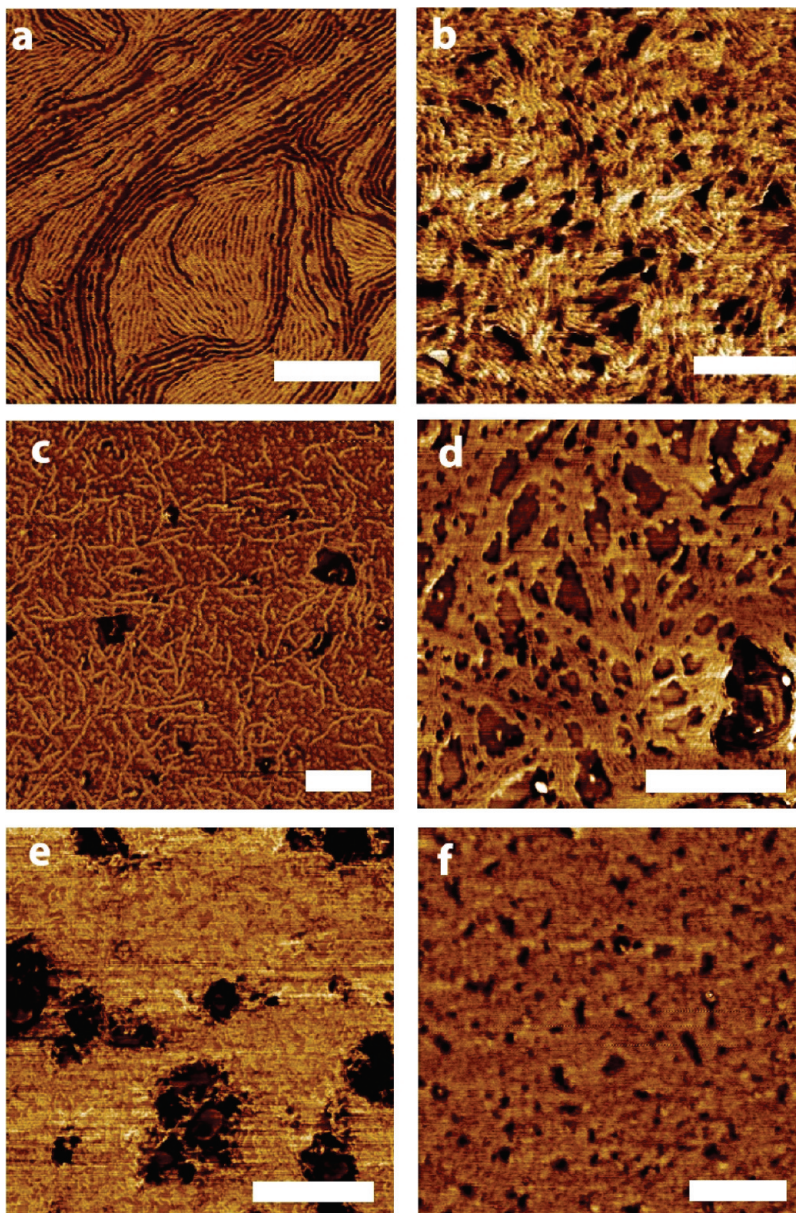


**Figure 7.** TM-AFM phase images of thin films of (a) the pure P3HT–OH macroinitiator, (b) the P3HT-*b*-PLLA copolymer, (c) the P3HT-*b*-PLLA/P3HT-*b*-PDLA stereocomplex, (d) a mixture of P3HT-*b*-PLLA and PLLA, (e) the P3HT-*b*-PLLA/PDLA stereocomplex, and (f) the pure PDLA homopolymer. The white scale bars in the bottom right corners of the images are 250 nm long.

## Conclusion

In summary, poly(3-hexylthiophene)-*b*-poly(L-lactide) and poly(3-hexylthiophene)-*b*-poly(D-lactide) block copolymers were successfully synthesized via a three-step procedure including the use of metal-free organic catalysts in the ring-opening polymerization of L- and D-lactide. The interest of these diblock copolymers relies upon the presence of a polylactide block that is able to form stereocomplex even in the presence of a regioregular poly(3-hexylthiophene) block. The thermal, crystalline, and microscopic morphology properties of stereocomplexed P3HT-*b*-PLA diblock copolymers were evaluated by DSC, XRD, and AFM. Stereocomplexation was confirmed also by the formation of stereocomplexes between a high-molecular-weight PDLA homopolymer and the P3HT-*b*-PLLA block copolymer. The forces driving the PLA stereocomplex formation are able to suppress the long-range ordered fibrillar structure of P3HT and to form nanoscale PLA domains, which after selective etching and successful filling with electron acceptor compound could lead

to novel nanostructured materials for bulk heterojunction organic solar cell devices.

**Acknowledgment.** This work was supported by the European Commission and Région Wallonne FEDER program (Materia Nova) and OPTI<sup>2</sup>MAT program of excellence, by the Interuniversity Attraction Pole program of the Belgian Federal Science Policy Office (PAI 6/27), and by FNRS-FRFC. The authors thank Mr. Julien De Winter and Dr. Pascal Gerbaux for assistance in the MALDI-ToF analysis. O.C. and M.S. are Research Associates of FNRS.

**Supporting Information Available:** General methods, materials, synthesis of homopolymers, and XRD analyses. This material is available free of charge via the Internet at <http://pubs.acs.org>.

## References and Notes

- (1) McCullough, R. D. *Adv. Mater.* **1998**, *10*, 93–116.
- (2) Schilinsky, P.; Asawapirom, U.; Scherf, U.; Biele, M.; Brabec, C. *Chem. Mater.* **2005**, *17*, 2175–2180.

- (3) Osaka, I.; McCullough, R. D. *Acc. Chem. Res.* **2008**, *41*, 1202–1214.
- (4) Sirringhaus, H.; Tessler, N.; Friend, R. H. *Science* **1998**, *280*, 1741–1744.
- (5) Wang, G.; Swensen, J.; Moses, D.; Heeger, A. J. *J. Appl. Phys.* **2003**, *93*, 6137–6141.
- (6) Sirringhaus, H. *Adv. Mater.* **2005**, *17*, 2411–2425.
- (7) Panzer, M. J.; Frisbie, C. D. *Adv. Funct. Mater.* **2006**, *16*, 1051–1056.
- (8) Padinger, F.; Rittberger, R. S.; Saraciftci, N. S. *Adv. Funct. Mater.* **2003**, *13*, 85–88.
- (9) Li, G.; Shrotriya, V.; Huang, J.; Yao, Y.; Moriarty, T.; Emery, K.; Yang, Y. *Nature Mater.* **2005**, *4*, 864–868.
- (10) Kim, J. Y.; Lee, K.; Coates, N. E.; Moses, D.; Nguyen, T.; Dante, M.; Heeger, A. J. *Science* **2007**, *317*, 222–225.
- (11) Heremans, P.; Cheyns, D.; Rand, B. P. *Acc. Chem. Res.* **2009**, *42*, 1740–1747.
- (12) Sundararaman, A.; Victor, M.; Varughese, R.; Jakle, F. *J. Am. Chem. Soc.* **2005**, *127*, 13748–13749.
- (13) Grimsdale, A. C.; Chan, K. L.; Martin, R. E.; Jokisz, P. G.; Holmes, A. B. *Chem. Rev.* **2009**, *109*, 897–1091.
- (14) Sugimoto, R.; Takeda, S.; Gu, H. B.; Yoshino, K. *Chem. Express* **1986**, *1*, 635–638.
- (15) Hotta, S.; Soga, M.; Sonoda, N. *Synth. Met.* **1988**, *26*, 267–279.
- (16) Hotta, S.; Rughooputh, S. D. D. V.; Heeger, A. J.; Wudl, F. *Macromolecules* **1987**, *20*, 212–215.
- (17) McCullough, R. D.; Lowe, R. D. *J. Chem. Soc., Chem. Commun.* **1992**, *1*, 70–72.
- (18) Chen, T. A.; Rieke, R. D. *J. Am. Chem. Soc.* **1992**, *114*, 10087–10088.
- (19) Loewe, R. S.; Khersonsky, S. M.; McCullough, R. D. *Adv. Mater.* **1999**, *11*, 250–253.
- (20) Jeffries-EL, M.; Sauve, G.; McCullough, R. D. *Adv. Mater.* **2004**, *16*, 1017–1019.
- (21) Jeffries-EL, M.; Sauve, G.; McCullough, R. D. *Macromolecules* **2005**, *38*, 10346–10352.
- (22) McCullough, R. D.; Tristram-Nagle, S.; Williams, S. P.; Lowe, R. D.; Jayaraman, M. *J. Am. Chem. Soc.* **1993**, *115*, 4910–4911.
- (23) Chen, T. A.; Wu, X.; Rieke, R. D. *J. Am. Chem. Soc.* **1995**, *117*, 233–244.
- (24) Liu, J.; Arif, M.; Zou, J.; Khondaker, S. I.; Zhai, L. *Macromolecules* **2009**, *42*, 9390–9393.
- (25) Sauve, G.; McCullough, R. D. *Adv. Mater.* **2007**, *19*, 1822–1825.
- (26) Iovu, M. C.; Craley, C. R.; Jeffries-EL, M.; Krankowski, A. B.; Zhang, R.; Kowalewski, T.; McCullough, R. D. *Macromolecules* **2007**, *40*, 4733–4735.
- (27) Iovu, M. C.; Jeffries-EL, M.; Sheina, E. E.; Cooper, J. R.; McCullough, R. D. *Polymer* **2005**, *46*, 8582–8586.
- (28) Iovu, M. C.; Jeffries-EL, M.; Zhang, R.; Kowalewski, T.; McCullough, R. D. *J. Macromol. Sci., Part A: Pure Appl. Chem.* **2006**, *43*, 1991–2000.
- (29) Dai, C.; Yen, W.; Lee, Y.; Ho, C.; Su, W. *J. Am. Chem. Soc.* **2007**, *129*, 11036–11038.
- (30) Liu, J.; Sheina, E.; Kowalewski, T.; McCullough, R. D. *Angew. Chem., Int. Ed.* **2002**, *41*, 329–332.
- (31) Craley, C. R.; Zhang, R.; Kowalewski, T.; McCullough, R. D.; Stefan, M. C. *Macromol. Rapid Commun.* **2009**, *30*, 11–16.
- (32) Boudouris, B. W.; Frisbie, C. D.; Hillmyer, M. A. *Macromolecules* **2008**, *41*, 61–75.
- (33) Botiz, I.; Darling, S. B. *Macromolecules* **2009**, *42*, 8211–8217.
- (34) Ikada, Y.; Tsuji, H. *Macromol. Rapid Commun.* **2000**, *21*, 117–132.
- (35) Tsuji, H. In *Polyesters 3*; Doi, Y., Steinbuchel, A., Eds.; Wiley-VCH: Weinheim, 2002; Vol. 4, p 129.
- (36) Pachence, J.; Kohn, J. In *Principle of Tissue Engineering*, 2nd ed.; Lanza, R., Langer, R., Vacanti, J., Eds.; Academic Press: San Diego, 2000; p 263.
- (37) Ma, P. *Mater. Today* **2004**, *7*, 30–40.
- (38) Xiang, Z.; Sarazin, P.; Favis, B. D. *Biomacromolecules* **2009**, *10*, 2053–2066.
- (39) Auras, R.; Harte, B.; Selke, S. *Macromol. Biosci.* **2004**, *4*, 835–864.
- (40) Ikada, Y.; Jamshidi, K.; Tsuji, H.; Hyon, S.-H. *Macromolecules* **1987**, *20*, 904–906.
- (41) Tsuji, H. *Macromol. Biosci.* **2005**, *5*, 569–597.
- (42) Okihara, T.; Tsuji, M.; Kawaguchi, A.; Katayama, K.-I.; Tsuji, H.; Hyon, S.-H.; Ikada, Y. *J. Macromol. Sci., Part B: Phys.* **1991**, *30*, 119–140.
- (43) Brizzolara, D.; Cantow, H.-J.; Diederichs, K.; Keller, E.; Domb, A. J. *Macromolecules* **1996**, *29*, 191–197.
- (44) Dowe, A. P. *Chem. Commun.* **2008**, *48*, 6446–6470.
- (45) Loewe, R. S.; Ewbank, P. C.; Liu, J.; Zhai, L.; McCullough, R. D. *Macromolecules* **2001**, *34*, 4324–4333.
- (46) Yokoyama, A.; Miyakoshi, R.; Yokozawa, T. *Macromolecules* **2004**, *37*, 1169–1171.
- (47) Miyakoshi, R.; Yokoyama, A.; Yokozawa, T. *J. Am. Chem. Soc.* **2005**, *127*, 17542–17547.
- (48) Iovu, M. C.; Sheina, E. E.; Gil, R. R.; McCullough, R. D. *Macromolecules* **2005**, *38*, 8649–8656.
- (49) Parakka, J. P.; Cava, M. P. *Tetrahedron* **1995**, *51*, 2229–2242.
- (50) Liu, J.; Loewe, R. S.; McCullough, R. D. *Macromolecules* **1999**, *32*, 5777–5785.
- (51) Pratt, R. C.; Lohmeijer, B. G. G.; Long, D. A.; Waymouth, R. M.; Hedrick, J. L. *J. Am. Chem. Soc.* **2006**, *128*, 4556–4557.
- (52) Lohmeijer, B. G. G.; Pratt, R. C.; Leibhart, F.; Logan, J. W.; Long, D. A.; Dove, A. P.; Nederberg, F.; Choi, J.; Wade, C.; Waymouth, R. M.; Hedrick, J. L. *Macromolecules* **2006**, *39*, 8574–8583.
- (53) Tsuji, H.; Hyon, S.-H.; Ikada, Y. *Macromolecules* **1991**, *24*, 5651–5656.
- (54) Bouapao, L.; Tsuji, H. *Macromol. Chem. Phys.* **2009**, *210*, 993–1002.
- (55) Tsuji, H.; Okumura, A. *Macromolecules* **2009**, *42*, 7263–7266.
- (56) Sarasua, J.-R.; Prud'homme, R. E.; Wisniewsky, M.; Le Borgne, A.; Spassky, N. *Macromolecules* **1998**, *31*, 3895–3905.
- (57) Tsuji, H.; Horii, F.; Nakagawa, M.; Ikada, Y.; Odani, H.; Kitamaru, R. *Macromolecules* **1992**, *25*, 4114–4118.
- (58) Prosa, T. J.; Winokur, M. J.; Moulton, J.; Smith, P.; Heeger, A. J. *Macromolecules* **1992**, *25*, 4364–4372.
- (59) Sugiyama, K.; Kojima, T.; Fukuda, H.; Yashiro, H.; Matsuura, T.; Shimoyama, Y. *Thin Solid Films* **2008**, *516*, 2691–2694.
- (60) Zhang, R.; Li, B.; Iovu, M. C.; Jeffries-EL, M.; Sauve, G.; Cooper, J.; Jia, S.; Tristram-Nagle, S.; Smilgies, D. M.; Lambeth, D. N.; McCullough, R. D.; Kowalewski, T. *J. Am. Chem. Soc.* **2006**, *128*, 3480–3481.
- (61) Surin, M.; Coulembier, O.; Tran, K.; De Winter, J.; Leclere, P.; Gerbaux, P.; Lazzaroni, R.; Dubois, P. *Org. Electron.* **2010**, *11*, 767–774.